Environmental Science and Pollution Research (2023) 30:108706–108719
https://doi.org/10.1007/s11356-023-30046-1

RESEARCH ARTICLE

Improving the adsorption performance of non-polar benzene vapor by using lignin-based activated carbon

Kaan Isinkaralar[1]

Received: 3 July 2023 / Accepted: 19 September 2023 / Published online: 26 September 2023

Abstract

Both indoor and outdoor contamination continually contain benzene vapor. It has primary concerns about long-term health risks to the living environment. Benzene is a crucial airborne pollutant in the environment due to its apparent acute toxicity, high volatility, and poor degradability. It is especially urgent to restrain benzene emissions due to the persistent concentration increase and stringent processes. Benzene adsorption is a highly efficient mechanism with low cost, low energy consumption, and a simple process. In this study, biomass-derived porous carbon materials (TCACs) were synthesized by pyrolysis activation combined with H_3PO_4, HNO_3, and HCl. TCAC44 has the best activation conclusion, showing that surface area and pore volume were 1107 m^2/g and 0.58 cm^3/g treated with H_3PO_4 and so was chosen for subsequent benzene adsorption/desorption tests. The adsorption capacities of benzene for TCAC44 were increased from 58 mg/g for 35 °C + 95% RH to 121 mg/g for 25 °C + 15% RH and presented a higher adsorption capacity of benzene than TCAC101 and TCAC133. Otherwise, well recyclability of TCAC44 was revealed as the benzene adsorption capacity reductions were 22.49% after five adsorption-desorption cycles. Furthermore, the present study established the property-application relationships to promote and encourage future research on the newly synthesized innovative TCAC44 for benzene removal.

Keywords Volatile organic compounds (VOCs) · Porous carbon · Structure effect · Sustainable manufacturing

Introduction

Benzene (C_6H_6) is a non-polar deleterious contaminant among aromatic volatile organic compounds (VOCs) released by residential, urbanization, and industrial sources which are ongoing global problems to the atmosphere (Spinelle et al. 2017). Benzene is one of the most familiarly used solvents and a major air pollutant today, which participates in atmospheric photochemical reactions as precursor gaseous (Szulejko et al. 2019). Exposure to this substance, which is very easy to change from liquid to gaseous, can be severe and dangerous to the ecological environment and human health (Rich and Orimoloye 2016; Sun et al. 2018a; Isinkaralar 2023a). Benzene exposure is announced in the carcinogen capability to humans that it has been graded as Group 1 by the International Agency for Research on Cancer (IARC 1987). The Occupational Safety and Health Administration (OSHA) emphasized the importance of the effects on the workplace people determined the short-term exposure limit values as 1 ppm (3.25 mg/m^3) as an 8 h mean or 5 ppm for 15 min (OSHA 1987), and the European Union (EU) has decided an annual limit of 5 µg/m^3 for gaseous benzene exposure (European Directive 2008/50/EC) due to that 99% of the world's population lives in polluted air that does not encounter the WHO recommendation (WHO 2021).

Benzene, commonly found in the indoor and outdoor atmosphere, causes significant amounts of release at various concentrations from there to ambient environment (Baberi et al. 2022; Singh et al. 2023). Among these sources, the petroleum refineries (Bayatian et al. 2021), the petrochemical industry (Jephcote and Mah 2019), gas stations (Hsieh et al. 2021), coal combustion (Fan et al. 2014), traffic arteries (Alfoldy et al. 2019), industrial solvents (Luijten et al. 2020), domestic care products (Du et al. 2014), building-related materials (Zhang et al. 2018), and cigarette smoke (Antonucci et al. 2020) are attributed to large quantities of

Responsible Editor: Tito Roberto Cadaval Jr

✉ Kaan Isinkaralar
kisinkaralar@kastamonu.edu.tr

[1] Department of Environmental Engineering, Faculty of Engineering and Architecture, Kastamonu University, 37150 Kastamonu, Türkiye

benzene emission for the atmospheric environment. The dominant benzene has caused health problems including nausea, eye and throat irritation (Tunsaringkarn et al. 2012), asthma attacks (Orru et al. 2018), headache, dizziness, and fatigue (Norbäck et al. 2017), cognitive confusion (Hu et al. 2021), acute leukemia (Janitz et al. 2017), and hematotoxicity (Ren et al. 2022).

People ordinarily spend more than 19 h of daily time in indoor areas where indoor air quality is affected by benzene emission from several sources (Liu et al. 2020). Especially benzene is a significant contributor to poor indoor air quality. Therefore, air change allows extraction and dilution to reduce the benzene amounts from indoor sources (Sun et al. 2019; Fan et al. 2022). However, if the ventilation is insufficient to balance indoor emissions, some control approach should be individually considered for reduced emissions (Ye et al. 2017; Deng et al. 2021). The benzene pollution control technologies significantly challenge defending environmental health with recovery and destruction mechanisms.

Benzene reacts with other air pollutants to be transformed into various types of byproducts, such as biphenyl, anthracene, naphthalene, and pyrene, which can assist to haze formation in the atmosphere (Ji et al. 2020; Chu et al. 2021). The removal of benzene, which has a liquid or gaseous form, has been tried using various methods and techniques. In light of the environmental and health hazards of benzene, there are different sustainable techniques such as catalytic combustion (Yang et al. 2017), membrane (Ge and Choi 2017), catalytic technologies (Zhao et al. 2023), nonthermal plasma (Jiang et al. 2018), catalytic oxidation (Huang et al. 2016), UV-ozone technology (Oliva et al. 2022), photocatalytic oxidation (Kang et al. 2018), biofiltration (Rajamanickam et al. 2020), and adsorption (Isinkaralar 2023b). Among these options, adsorption has been suggested as a promising option as high efficiency and low cost to reducing benzene emissions without secondary pollution if performed successfully. There are different application routes used for gaseous benzene by considering adsorption. Typically, the adsorbents used are MOF (Xie et al. 2018), biochar (Vikrant et al. 2020), silica (Alipour et al. 2021), activated carbon (Shi et al. 2022), modified activated carbon (Zhou et al. 2019), hollow carbon spheres (Chen et al. 2023), diatomite (Khalighi Sheshdeh et al. 2013), and zeolites (Yu et al. 2015) to achieve efficient adsorption of benzene (Li et al. 2020). Besides, types of carbon-based adsorbent applications have been made to develop benzene adsorption with economic feasibility, simplicity, and effectiveness.

Over the last few decades, gas adsorption has been investigated preferentially for carbon-based adsorbent materials depending on a large extent on their amount, type, positioning, and surface properties of the loaded which should be well known in the removal of gaseous benzene (Zhang et al. 2017; Zhu et al. 2020; Kumar et al. 2023). Although its applications to investigate its efficiency in benzene removal are quite common, it is still researching a hot and famous topic on air quality. The principal reason is to reduce the cost, increase efficiency, and increase adaptability to daily life. Therefore, the preferred biogenic raw materials for adsorbent are forestry and agricultural residues (Mao et al. 2016; Seku et al. 2019; Kadimpati et al. 2020; Zhu et al. 2021). In particular, materials with lignin-containing structure, no economic value, difficult and non-reusable materials, and massive amounts have mainly been preferred for promising feedstocks for producing ACs (Kadimpati et al. 2021).

The great potential of lignocellulosic waste with chemical activation has been chosen to develop a carbon-adsorbent that can efficiently treat gaseous benzene with better porous structure using the most common chemicals such as $ZnCl_2$, KOH, H_3PO_4, and K_2CO_3 (Mohammed et al. 2015). Despite its ecologic and economic value, wastes are generated with extreme climatic events such as summer droughts and heat waves, which cannot be evaluated for functionality in forest and ecological management. *Tilia cordata* has also emerged potential precursor for the production of carbon-based adsorbents in environmental approaches (De Jaegere et al. 2016). It is a forestry byproduct, has a lignin structure, and can be found as renewable plant feedstocks for the formation of pyrolyzed, which has the most remarkable effect followed by the heating rate, the nitrogen stream rate, and the duration (Ansari et al. 2022; Gayathiri et al. 2022). In doing so, the basic components of *T. cordata* include lignin, which tends to produce nonporous graphitic carbon, hemicellulose for eliminating other compounds, and cellulose for graphite formation, effectively contributing to the adsorbent structure.

The study hopes to assist in decreasing gaseous benzene concentrations in producing activated carbon using *T. cordata*. It was investigated, and the removal efficiency at different concentrations with the activated carbons with a high surface area was investigated due to the potentially harmful effects of contaminated air which are the most serious and essential for life, and air quality dramatically affects people's health. Optimum performance was achieved by changing the amount of activated carbon in line with the data obtained. The aim of this paper was to assess the performance of TCAC44, TCAC101, and TCAC133 as effective benzene sorbents, to analyze the effects of H_3PO_4 HNO_3, and HCl activation on the benzene adsorption capacity of TCAC44, TCAC101, and TCAC133 and to show the benzene adsorption-desorption mechanisms.

Material and methods

Synthesis of TCACs

In this study, *Tilia cordata* residues (TCRs) were obtained at a local forest of Kastamonu, Türkiye, and have been used

as a biomass precursor for the production of activated carbon (TCACs). The TCRs were first cleaned with deionized water and dried for several days at 55 °C for 2 weeks to remove any surface moisture. Then they were crushed and sieved to reduce the size to 2–3-mm diameter for the next step. The acid solutions were prepared to the desired impregnation ratios of 1.0, 2.0, and 3.0, defined as the ratio of the dry weight of acid solutions to the weight of the TCR powder. Twenty to 60 g of the precursor was used per sample, and dried powder was dissolved in 250 mL of distilled water. Then the solids were impregnated with H_3PO_4, HNO_3, and HCl which were stirred at approximately 150 ±4 °C for 20 min to ensure a whole reaction between chemicals and TCR powder.

The soaking time at room temperature for 24 h and 20 g of the impregnated sample was placed on a ceramic crucible into a carbonization reactor in a tubular furnace (Carbolite, CTF 1200) with a programmable controller under the N_2 flow. The tubular furnace was started with a heating rate of 10 °C/min to a final temperature of 450, 550, 650, 750, 850, and 950 °C and (an accuracy of ±5°C) kept at 60, 90, and 120 min, respectively, at this temperature in the ratio of 100 cm^3/min N_2 gas flow. The N_2 atmosphere continued until the samples were cold, and took out the cooled samples for washing until the pH reading was at 6–7. They were washed with 0.1 M sodium hydroxide (NaOH) solution and cleaned using boiling deionized water. Then washed TCACs were dried in an oven with a temperature set at 105 °C for 48 h and were named "TCAC1," "TCAC2," and "TCAC3 until TCAC162" based on their ratios before benzene adsorption experiments in Table 1. All chemical agents used for the TCACs production, including H_3PO_4, HNO_3, HCl, C_6H_6, and all other reagents, were analytical grade by Sigma-Aldrich.

The yield of TCACs was calculated using Eq. 1 as the mean of three tests by standard deviations (Liu et al. 2021).

$$Yield\ of\ TCAC\ (wt\%) : \frac{Final\ weight\ of\ TCAC}{Initial\ weight\ of\ \mathrm{TCR}} \times 100 \quad (1)$$

Characterization of the TCAC preparation

The morphologies of the TCR and TCACs were assessed in contents of carbon, hydrogen, and nitrogen using a EuroVector, EA3000 Single elemental analyzer with ±0.3% accuracy (EuroVector, Italy), and oxygen contents were made an inference by the difference of others. In order to identify the surface area and the pore structure of TCACs, N_2 adsorption/desorption isotherms and pore size distribution at a temperature of −196 °C were quantified by DFT (density functional theory) method with an automated adsorption device Quantachrome-Autosorb-1C (Quantachrome Instruments, USA). Surface area, pore volume, and distribution were retrieved from N_2 adsorption measurements by Quantachrome computer software ($P/P_0 = 0.99$). TCACs were evaporated in the vacuum at 300 °C for 3 h and the visible surface area of N_2 was analyzed on a NOVA touch LX4 (Quantachrome,

Table 1 Carbonization and activation condition of TCACs

Impregnation ratio of the weight of the activating agents and precursor	Carbonization time (min)	Carbonization condition (°C)	Activating agent		
			H_3PO_4	HNO_3	HCl
1:1, 2:1, 3:1	60	450	TCAC1-3	TCAC55-57	TCAC109-111
1:1, 2:1, 3:1	60	550	TCAC4-6	TCAC58-60	TCAC112-114
1:1, 2:1, 3:1	60	650	TCAC7-9	TCAC61-63	TCAC115-117
1:1, 2:1, 3:1	60	750	TCAC10-12	TCAC64-66	TCAC118-120
1:1, 2:1, 3:1	60	850	TCAC13-15	TCAC67-69	TCAC121-123
1:1, 2:1, 3:1	60	950	TCAC16-18	TCAC70-72	TCAC124-126
1:1, 2:1, 3:1	90	450	TCAC19-21	TCAC73-75	TCAC127-129
1:1, 2:1, 3:1	90	550	TCAC22-24	TCAC76-78	TCAC130-132
1:1, 2:1, 3:1	90	650	TCAC25-27	TCAC79-81	TCAC133-135
1:1, 2:1, 3:1	90	750	TCAC28-30	TCAC82-84	TCAC136-138
1:1, 2:1, 3:1	90	850	TCAC31-33	TCAC85-87	TCAC139-141
1:1, 2:1, 3:1	90	950	TCAC34-36	TCAC88-90	TCAC142-144
1:1, 2:1, 3:1	120	450	TCAC37-39	TCAC91-93	TCAC145-147
1:1, 2:1, 3:1	120	550	TCAC40-42	TCAC94-96	TCAC148-150
1:1, 2:1, 3:1	120	650	TCAC43-45	TCAC97-99	TCAC151-153
1:1, 2:1, 3:1	120	750	TCAC46-48	TCAC100-102	TCAC154-156
1:1, 2:1, 3:1	120	850	TCAC49-51	TCAC103-105	TCAC157-159
1:1, 2:1, 3:1	120	950	TCAC52-54	TCAC106-108	TCAC160-162

USA) following the BET (Brunauer-Emmett-Teller) equation. Fourier transform infrared spectra (FTIR) of surface functional groups were characterized with the use of Perkin-Elmer TGA 7 (Waltham, MA). Surface morphologies were studied in Quanta FEG 250 (FEI, USA) by scanning electron microscopy (SEM). The decomposition processes of TCR and TCACs were determined using a thermal gravimeter analyzer (STA7300, Hitachi, Japan) under the N_2 ambient.

Experimental test procedure

The general experimental procedure with TCAC44 TCAC101 and TCAC133 as individual carbonaceous adsorbents were premixed at threshold concentrations of 10 to 200 mg/m^3 benzene. On one hand, 0.3 g of the TCAC44, TCAC101, and TCAC133 was used for each investigation under 35 and 95% RH for 70 min. For periodic sampling, a temperature-controlled batch reactor connected to a 50 mL/min N_2 flow rate as a surrogate gas, which allows the benzene to evaporate, following the mass balance of benzene steam, was directly collected into a Tenax®-TA single sorbent tube directly using a vacuum air pump (200 mL/min, AirLite 110-100, SKC, USA) as depicted in Fig. 1. Simply put, Tenax vials were subsequently tested and analyzed using thermal desorption (TD; Markes Unity Series 2, Markes International Ltd., Llantrisant, UK) in combination to a gas chromatography/mass spectrometry detector (GC-MS; Thermo Scientific Trace 1300 and ISQ-QD Thermo Fisher Scientific). A TG-624 capillary column (60 m × 0.25 mm ID × 1.4 µm film) for the thermal desorber was deployed to control compounds based on US EPA Method TO-17 (US EPA 1999). Experiments were repeated at least once under the same conditions to ensure that the differences in the test results calculated from Eq. 2 for TCAC44, TCAC101, and

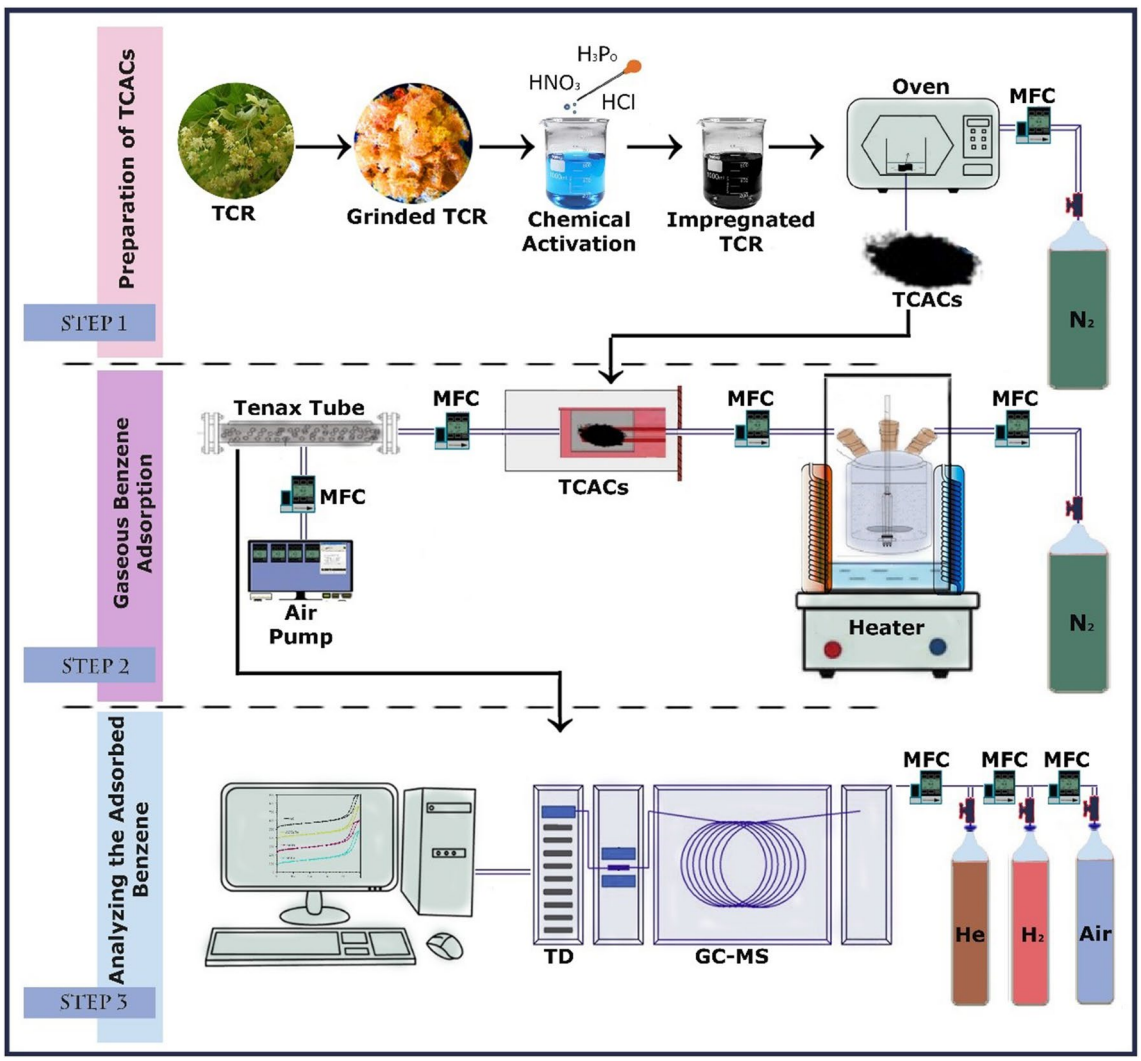

Fig. 1 Illustration of process steps in the benzene adsorption

TCAC133 were due to the amount of TCAC44, TCAC101, and TCAC133 rather than experimental errors. Rather than experimental errors, these are due to the amount of TCAC44 TCAC101 and TCAC133.

The benzene adsorption capacities were calculated with Eq. 2 (Isinkaralar 2023c).

$$q_{(mg/g)} = \left(\frac{F\ x\ C_0\ x\ 10^{-9}}{W}\right)\left[\left(\frac{C_i}{C_0}\ x\ t_s\right) - \left(\int_0^{t_s}\frac{C_i}{C_0}\ d_t\right)\right] \quad (2)$$

where q (mg/g) and t (min) represent saturated capacity and the time of benzene adsorption; C_0 and C_t (mg/m^3) display the inlet and outlet concentration of benzene at any time t; F (mL/min) and V (mg/m^3) show gas stream ratio and the benzene rate, and also m (g) corresponds to the mass of the TCACs.

Recyclability

This study intends to examine the benzene desorption tests performed on TCAC44 to search for recyclability. Inevitably, the single component adsorption had reached the equilibrium, and the desorption method was performed at 300 °C with a gas flow rate of 100 mL/min N_2 at 300 °C until no benzene was desorbed from TCAC44. Following the step, the adsorption was consecutively realized again as five cycles on TCAC44.

Results

Selection of the best TCACs

The result of proximate and elemental analyses of TCR, TCAC44, TCAC101, and TCAC133 is shown in Table 2. It is evident that the fixed carbon content percentage is higher in the TCACs than in the TCR, respectively. The fixed carbon, volatile matter, moisture, and ash contents were determined ASTM methods for TCR which were 16.27, 71.49, 10.43, and 1.81%, while the fixed carbon, volatile matter, moisture, and ash contents for TCAC44, TCAC101, and TCAC133 were 69.74, 68.59, and 65.77%; 23.70, 24.43, and 27.31%; 2.90, 3.40, and 2.10%; and 3.65, 3.58, and 4.82%. The TCR's moisture, ash, and volatile content are lesser than TCAC44, TCAC101, and TCAC133. The TCR has high volatile matter reduced from 71.49 to 23.70%. The decrease resulted from the carbonization and activation processes at high temperatures.

The fixed carbon was significantly enhanced from 16.27 to 69.74% due to effective physiochemical activations of their structure. The decrease in ash contents has seen that TCAC44, TCAC101, and TCAC133 are promising materials for benzene removal. Elemental content emerged with a comparable tendency with that of proximate analysis. The proportion of carbon (C) element in the precursor, TCR, increased from 27.63 to 78.05% given its suitable performance and efficiency for benzene treatment.

Hemicellulose, cellulose, and lignin contributed to the mass and the porous properties of TCACs. The lignocellulosic compositions of TRC are presented and the results showed that hemicellulose, cellulose, and lignin weight fractions were 14.7, 23.5, and 46.4%.

The large specific surface area and porosity surface remain significant features prompting the unique capability and efficacies of TCAC44, TCAC101, and TCAC133. This betterment on the mesopore surface area, BET surface area, average pore diameter, and total pore volume are displayed in Table 3. The TCAC44, TCAC101, and TCAC133 exhibit enhanced BET surface areas of 1107, 803, and 657 m^2/g and total pore volumes of 0.67, 0.48, and 0.39 cm^3/g. The notable rise in total pore volume and BET surface area were due to the runout of volatile matter and water from the TCR. The TCAC44, TCAC101, and TCAC133 exposited a mean pore diameter of 2.28, 1.89, and 1.84 nm, respectively.

The results of representative N_2 adsorption/desorption isotherms and pore size distribution of TCAC44, TCAC101, and TCAC133 are shown in Fig. 2a. The isotherms for all these TCACs were outgassed in vacuum at an ambient

Table 3 BET surface area and pore volumes of selected TCACs

Carbon ID	Yield (%)	S_{BET} (m^2/g)	V_{micro} (cm^3/g)	V_t (cm^3/g	D (nm)
TCAC44	75.9	1107	0.53	0.67	2.28
TCAC101	73.3	803	0.39	0.48	1.89
TCAC133	72.8	657	0.27	0.39	1.84

Table 2 Lignocellulosic compositions and proximate analyses of TCR and TACS

Material	Proximate analysis (w/w%)				Ultimate analysis (w/w%)			
	Moisture	Ash	Volatile matter	Fixed carbon	C	H	O	N
TCR	1.81	10.43	71.49	16.27	27.63	58.72	12.87	0.78
TCAC44	2.90	3.65	23.70	69.74	78.05	2.14	18.91	0.90
TCAC101	3.40	3.58	24.43	68.59	72.73	4.83	20.79	1.65
TCAC133	2.10	4.82	27.31	65.77	69.68	5.18	22.66	2.48

temperature of 300 °C for 5 h, and then showed a vertical increase in the amount of adsorbed N_2 with increasing order of relative pressure. Both the hysteresis cycle and the curve slope exhibited an S-shape and type IV isotherm at the onset of $P/P_0 \geq 0.45$ as per the International Union of Pure and Applied Chemistry (IUPAC) categorization. Type IV isotherm is defined by its hysteresis loop, associated with capillary condensation in the mesopore. The most critical textural changes caused by H_3PO_4, HNO_3, and HCl-activation were an increase in the micro/mesoporous network of the TCACs due to the splitting of particles (Oginni et al. 2019). The scope of such changes were dependent on the operating parameters (acid strength, temperature, duration, etc.) (Janković et al. 2019; Nasrullah et al. 2019).

The pore size distribution curves of the TCAC44, TCAC101, and TCAC133 are given in Fig. 2b. In a word, the dominant pore's diameter (d_p) was observed to fall between 0.5 and 5 nm, validating the excellent agreement to the mesoporous surface morphology of TCAC44, TCAC101, and TCAC133. Treatment with acid caused the creation of fewer pores in the rigid particles, leading to a greater total surface area. As a consequence, the H_3PO_4, HNO_3, and HCl-activation caused variation in the cumulative pore volume, which was responsible for the improvement of the adsorption properties of the TCAC44, TCAC101, and TCAC133, which led to an improvement in the porosity of the virgin material (Adan-Mas et al. 2021).

Figure 3 shows the scanning electron micrographs of prepared TCR, TCAC44, TCAC101, and TCAC133 under optimized conditions in which their surface morphology has visible cavities, crevices, pores, and holes of various sizes. The interaction between H_3PO_4, HNO_3, HCl, and carbon is also enhanced, forming well-developed pores. The TCR precursor is subjected to elevated irregular shapes in nature and the absence of porosity. Figure 3 b shows that the TCAC44 was somewhat monitored to possess many smooth pores over its surfaces. The TCAC133 and TCAC101 developed a small number of uniformly immobilized pores from the evaporation of the HCl and HNO_3 during carbonization. Thus, verifying its effectiveness of chemical activation combined with H_3PO_4 heating at 650 °C in preparing a well-developed and homogeneous structure of TCAC44 indicates that the activation process using HNO_3 has formed the widening aggregates and cavities of pores on the TCAC101 for fully enhanced experiments.

The functional group composition of TCR, TCAC44, TCAC101, and TCAC133 is shown in the FT-IR spectra in Fig. 4. Both spectra have similar properties and the adsorption peaks demonstrate complicated surface chemistry which plays a critical factor in gaseous benzene adsorption through Lewis acid–base interactions. The strong and broad band between 3322 and 3286 cm^{-1} of TCR, TCAC44, TCAC101, and TCAC133 can be nominated to O–H groups, carboxylic groups, or amide N–H stretching, corresponding to the vibration of functional groups in cellulose or hemicellulose (Danish et al. 2014). There is a clear band around 2879 cm^{-1} which is reported to be symmetric or asymmetric stretching vibrations of C–H bonds in CH_2 and CH_3 groups. The relatively intense bands at 1617 cm^{-1} were attributed to the stretching vibration of C=O in carboxylic acids, and the band intensity was reduced in TCAC44.

The intense band around 1520 cm^{-1} confirmed olefins and skeletal vibrations in the aromatic structures related to C=C vibrations (Rashid et al. 2019). The decreased adsorption of small peaks with oxidized carbons in TCAC113 at 1118 cm^{-1} was caused by the stretching vibration of C=O in phenols, alcohols, acids, ethers, and esters (Reffas et al. 2010). The C–H and C–O cellulose bands in TCAC44, TCAC101, and TCAC133 could be observed from 1150 to 937 cm^{-1}, and the damaged cellulose structure might cause decreased intensity. The intensity of absorption peaks at 1617 and 983 cm^{-1} appear to be the presence of C=O, aromatic C=C, and the symmetric stretching C–O–C, and the bands centered at 1399 cm^{-1} and 867 cm^{-1} are assigned to the C–N and N–H groups (Djilani et al. 2012). FT-IR spectra revealed that the conversion resulting in intensity change and peak shift and the functional groups (amine groups) were charged successfully on TCAC44, TCAC101, and TCAC133.

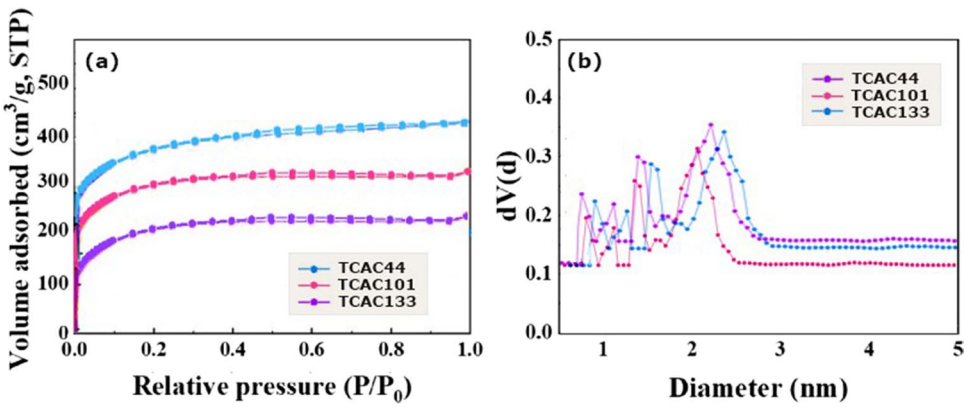

Fig. 2 N_2 adsorption/desorption isotherm (**a**) and pore diameter distribution patterns (**b**) of the TCAC44, TCAC101, and TCAC133

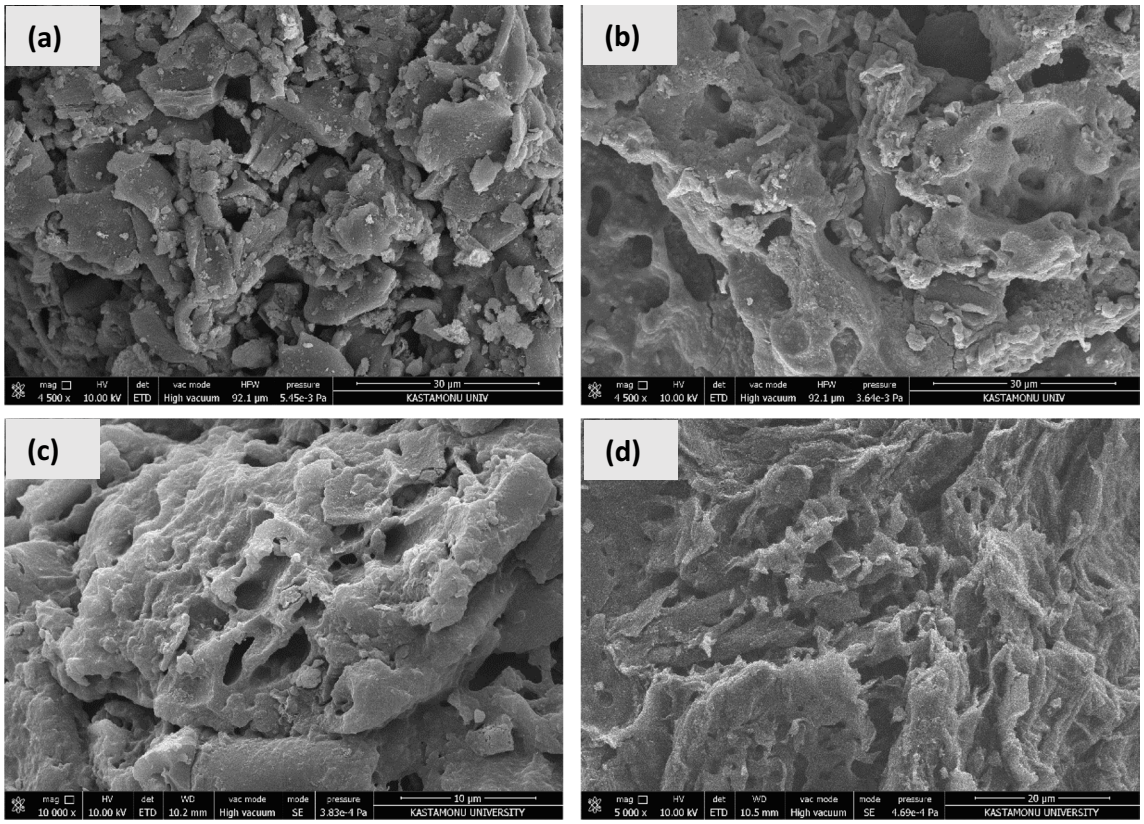

Fig. 3 Scanning electron micrographs of **a** TCR, **b** TCAC44, **c** TCAC101, and **d** TCAC133

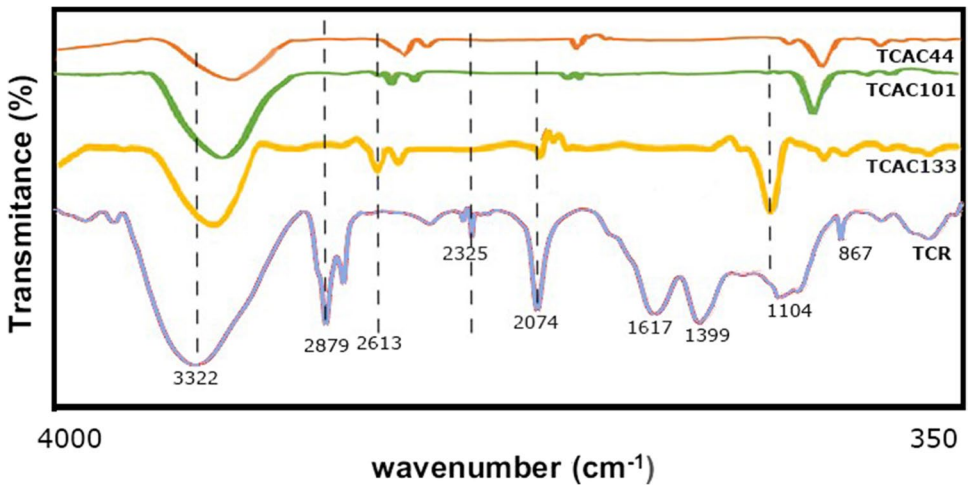

Fig. 4 FT-IR spectra of TCR, TCAC44, TCAC101, and TCAC133

TGA is beneficial in establishing the decomposition behavior and thermal stability of the experimental specimens, and the TGA curves of TCR, TCAC44, TCAC101, and TCAC133 are shown in Fig. 5. The weight loss of TG curves could be divided into three stages. The first stages appear by 25 to 235 °C for TCR, 95 to 385 °C for TCAC44, 90 to 360 °C for TCAC101, and 75 to 305 °C for TCAC133 due to the loss of water physisorbed about 10.26–13.20%, respectively (Gupta et al. 2022). The second stage started hemicellulose degradation at about 240 to 475 °C for TCR, 390 to 550 °C for TCAC44, 375 to 520 °C for TCAC101, and 310 to 515 °C for TCAC133.

The total weight losses of TCR, TCAC44, TCAC101, and TCAC133 were about 73.26, 35.69, 39.51, and 42.38% during pyrolysis. They were significant consecutive weight losses that the sharp exothermic degradation of cellulose, hemicellulose, or lignin mainly occurred for each TCACs (Tuli et al. 2020). The observable evolution profile of

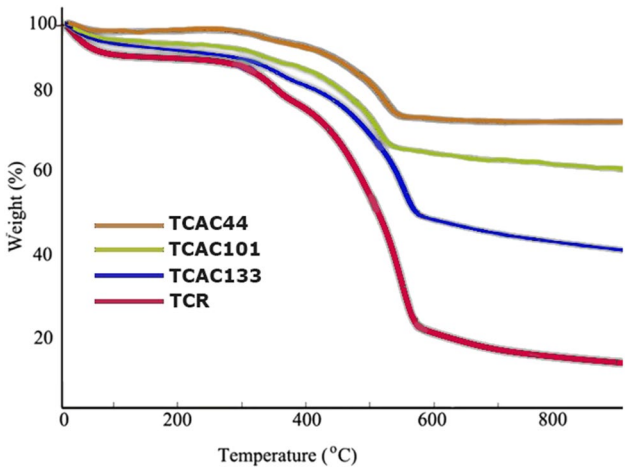

Fig. 5 TG curves of TCR, TCAC44, TCAC101, and TCAC133

480–630 °C was minimal in the third stage, indicating the presence of stable oxides at high temperatures. The critical degradation temperatures of TCR, TCAC44, TCAC101, and TCAC133 began at 235 °C, respectively, verifying that the modification reaction can enhance the stability of the compositions of the sample. Similarly, the devolatilization of several biomass is associated with the differences in the textural characterization of the samples (Ahmed et al. 2019).

Effect of different initial conditions of benzene adsorption

Differences in adsorption conditions revealed a remarkable difference in adsorption capacities. In particular, changes in temperature and humidity show variations in equilibrium conditions. Although the adsorbents used and their amounts are the same, the results are quite remarkable in Fig. 6. Benzene adsorption capacities for 25 °C are 121 mg/g at 15% RH, 93 mg/g at 42% RH, 81 mg/g at 76% RH, and 70 mg/g at 95% RH. The results here were found to be inversely correlated with relative humidity. Benzene in the pores was found notably in moisture and molecular. However, when the temperature is increased from 25 to 35 °C, it is seen that there is a severe decrease in the adsorption capacity. By keeping the same humidity values constant, by increasing the adsorption bed temperature, 85 mg/g at 15% RH, 76 mg/g at 42% RH, 67 mg/g at 76% RH, and 58 mg/g at 95% RH. In fact, it was clear from the amount it adsorbed that temperature and humidity play an essential role in its adsorption capacity.

Another critical parameter that affects the adsorption capacity is the waiting time. Figure 7 shows the effect of the lengthening or shortening of the time on the amount of adsorption. The performance obtained by exposing the adsorbents to different concentrations during the sampling period is given. In particular, the success of adsorbents increased the amount of adhesion, regardless of the concentration of the medium, as it began to adsorb from the first minute. Benzene adsorption efficiency for 25°C in the first 5 min was found as 25.71, 41.43, 55.71, and 70% at RH 15, 42, 76, and 95% respectively. Similarly at 35 °C in the first 5 min, it was recorded as 15.71, 30, 42.86, and 57.14% at RH 15, 42, 76, and 95% respectively. While the adsorption capacity of benzene reaches equilibrium in the first 25 min at 25 °C, this value comes after 38 min at 35 °C.

Recyclability

Benzene adsorption by TCAC44 is a simple and prevalent way in the mechanism. Nevertheless, the used TCAC44 would be a dangerous solid residue following the saturated sorption and thus its utilization should have low economic efficiency without being recycled. Thus, it is essential to check out the recyclability of the TCAC44. Thermal heating is extensively implemented to desorb benzene from TCAC44 and rescue invaded occupied pores. Figure 8 demonstrates the results of the calculation of adsorption capacities. After five adsorption/desorption cycle experiments, a very small decrease of 22.49% in benzene adsorption capacity was observed. Hence, 300 °C is a favorable heat

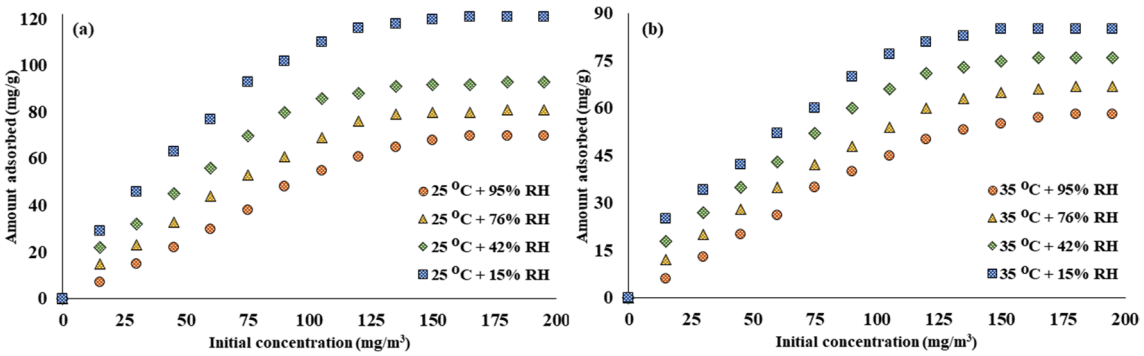

Fig. 6 Adsorption capacities of **a** 25 °C and **b** 35 °C

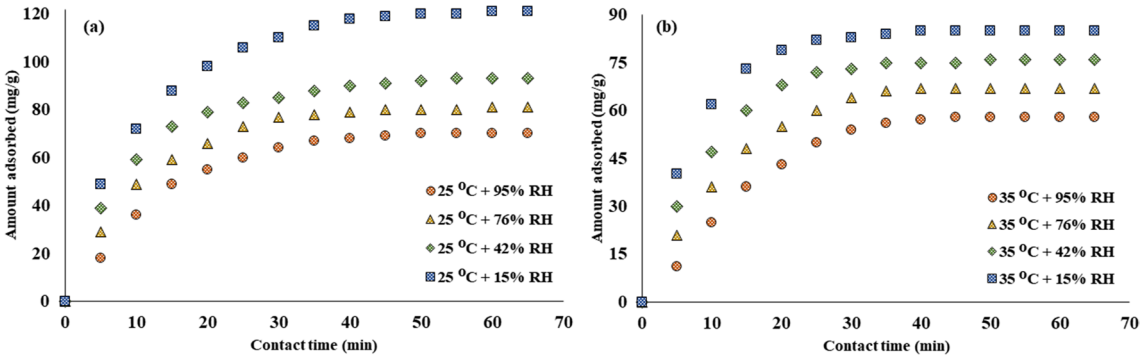

Fig. 7 Contact time of **a** 25 °C and **b** 35 °C

process conditions for the TCAC44 regeneration. Therefore, TCAC44 has excellent benzene recyclability and must be a high-quality adsorbent for efficient benzene removal in gaseous applications. Overall, the results confirm that the adsorption capacity of TCAC44 shows a downward trend from 121 to 93.79 mg/g, with a different degree of decline due to reducing the number of micropores serving as the leading reaction site for the benzene adsorption.

Discussion

In gaseous benzene in indoors, many societies are currently suffering from deteriorative impacts including climate change adaptation and urban/regional planning (Istanbullu et al. 2023; Isinkaralar and Varol 2023). An important point in the removal of benzene gas is the optimum adsorption application conditions, requiring planning through a long-term adsorptive approach. Benzene molecules are very active, and there may be differences according to the application area. Generally, the study on competitive adsorption of VOCs based on adsorbent differences (Zaitan et al. 2016), initial concentration-temperature-humidity (Laskar et al. 2019), single-multi component (Rajabi et al. 2021), and reactor types (Li et al. 2023) yields differences which were found during the sorption process (Trinh et al. 2016; Yao et al. 2020). It is to ensure that the adsorbents with the desired properties can be used repeatedly to remove benzene and other VOCs. In the studies, in adsorbents obtained from raw materials with lignocellulosic content, although the yield was found to be high at first, significant decreases were observed in subsequent loadings. This has created the need to increase the stability of the structure by highlighting the differences in the active carbon construction phase.

Porosity, micropore volume, and homogeneity in adsorbent structures are important stages of gas adsorption. The difference in the activation agents used in the production stage is the key functions that directly affects the formation

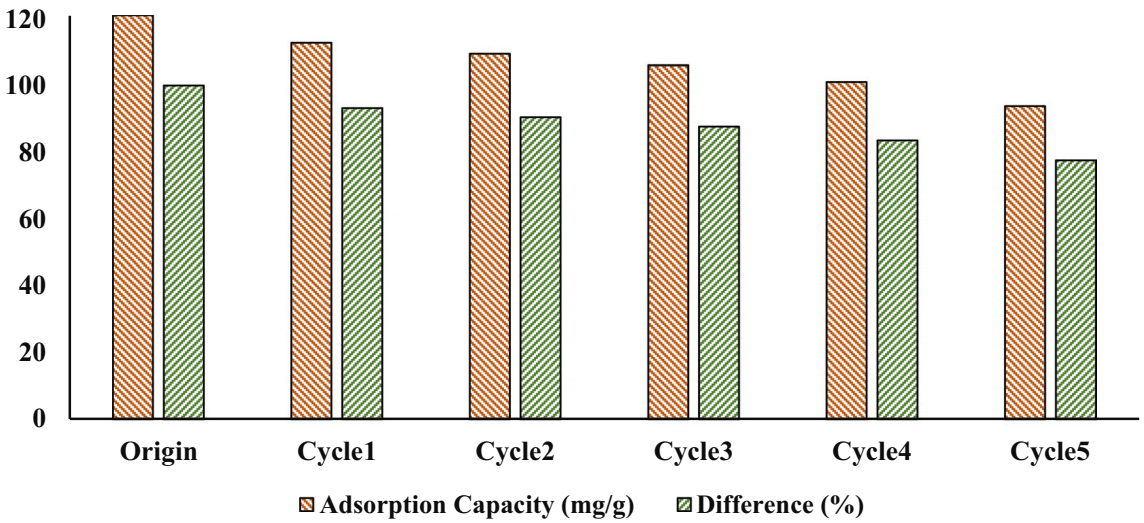

Fig. 8 Adsorption–desorption profiles of TCAC44

in the pores (Singuru et al. 2016; Sarkar et al. 2019; Paul et al. 2020; Boro et al. 2023). In studies conducted in this context, the difference of adsorbents has shown various successes in benzene removal efficiency. From existing literature, Vohra (2015) successfully prepared GAC (S_{BET}: 822 m^2/g and V_m: 0.346 cm^3/g) from palm date pits by chemical activation for gas-phase benzene adsorption. The benzene gas stream flow rate of 1.1 L/min as a total of 23 ppmv passed through the GAC-packed column at room temperature. The column breakthrough time displayed that saturated points were obtained between 774 and 951 min. Wang et al. (2015) synthesized OMC using the EISA route to investigate the static adsorption properties of benzene. The adsorption temperature was arranged at 25, 35, and 45 °C, and benzene was reached at 17.34, 16.86, and 16.71 mmol/g. In our research, the maximum adsorption amount was obtained at 25 °C and was reduced at 35 °C. Evidently, the adsorption of benzene gradually decreased with increasing temperature, indicating the adsorption mechanism's physical nature.

Liu et al. (2016) compared hydrophobic-modified PDMS as new porous materials with commercially bare-AC for benzene adsorption. The difference in adsorption capacity was more notable for PDMS/AC-150 and PDMS/AC-250 when the relative humidity increased to 50 and 90% RH. The water vapor adsorption capacities of PDMS/AC-150 and PDMS/AC-250 at a 50% RH were 56.4 ± 5.3 and 8.7 ± 0.3 mg/g. Similar to the findings under several relative humidities, TCAC44 showed a significant decrease with 95% RH. Some researchers deemed the conventional models for the description of adsorption isotherms of benzene onto activated carbon (Ushiki et al. 2015; Wjihi et al. 2017); however, these models are insufficient to describe exactly the adsorption behavior due to the lack of quantitative discussions about physic-chemical factors, such as temperature, humidity, and relation of adsorbate-adsorbent features on the fitting model (Konggidinata et al. 2017). Previous studies focused on the development of high-efficiency adsorbents for the enhanced gaseous stream of benzene, which was analyzed under the equilibrium conditions by Sun et al. (2018b), Jafari et al. (2018), and Rubahamya et al. (2019), although the activated carbon from lignocellulosic biomass is widely used and an important approach in benzene control with the developed microporous structure and favorable pore size. Bedane et al. (2019) reported high adsorption capacities for adsorption of ethyl benzene, toluene, and p-xylene from air streams using the prepared AC (S_{BET}: 1025 m^2/g and V_t: 0.49 cm^3/g) from peanut shell using $ZnCl_2$. Ha et al. (2020) purchased granular activated carbon (S_{BET}: 936.8 m^2/g of GAC) for PAC (S_{BET}: 956 m^2/g) preparation to explore the surface and diffusion adsorption mechanisms of benzene within the Bohart–Adam (B-A) model. They compared the removal performance 200 mg of GAC and PAC, which the intraparticle diffusion induced to the higher performance of GAC over PAC compared to the film mass transfer process.

TCAC44 exhibited similar adsorption performances with GAC and PAC, in which the benzene molecules have driven into most porous zones at higher flow rates. With the advent of an effective capturing strategy in benzene, the purification system of adsorption onto carbon-based materials from lignocellulosic biomass has been recognized from the reported literature (Wang et al. 2021; Yu et al. 2021; Valencia et al. 2022; Wang et al. 2022). Moreover, the research on the carbonaceous materials showed good operational stability between 4 and 6 cycles due to regenerating and reusing understanding for eco-friendly, cost, and energy-saving approaches. On the other hand, the total adsorption capacity achieved during the benzene adsorption also showed the TCAC44 was highly stable for the gas separation.

Conclusion

Benzene, which has a carcinogenic effect among the substances revealed in studies on indoor air quality, is quite dangerous at room temperature under normal conditions. TCAC44 has been produced from *T. cordata* as a low-cost, effortless, highly reusable, efficient, and human health biofilter. The competitive adsorption behaviors of TCAC44 indicate that 25 °C + 15% RH could reach adsorption equilibrium faster than other conditions. Temperature and relative humidity have a non-linear relationship with the adsorbed amount of benzene. The highest adsorption capacity of benzene onto TCAC44 at 25 °C + 15% RH was 121 mg/g. Success has been achieved by examining the holding capacity of benzene gas at different concentrations and conditions of this bio-adsorbent. Especially in ambient conditions, TCAC44 was found quite reasonable to use and showed an effective result. Additionally, the recyclability of adsorption further validated that TCAC44 is an economically feasible material for gas applications. In fact, it is expected to be a source of inspiration for researchers to remove other volatile organic compounds, equitably protect the indoor air in the future.

Author contribution This study is written entirely by Kaan Isinkaralar.

Data availability The data is provided by corresponding author under reasonable requests.

Declarations

Competing interests The author declares no competing interests.

Consent to publish Not applicable.

Ethics approval and consent to participate Not applicable.

References

Adan-Mas A, Alcaraz L, Arévalo-Cid P, López-Gómez FA, Montemor F (2021) Coffee-derived activated carbon from second biowaste for supercapacitor applications. Waste Manag 120:280–289. https://doi.org/10.1016/j.wasman.2020.11.043

Ahmed MB, Johir MAH, Zhou JL, Ngo HH, Nghiem LD, Richardson C, Moni MA, Bryant MR (2019) Activated carbon preparation from biomass feedstock: clean production and carbon dioxide adsorption. J Clean Prod 225:405–413. https://doi.org/10.1016/j.jclepro.2019.03.342

Alfoldy B, Mahfouz MMK, Yigiterhan O, Safi MA, Elnaiem AE, Giamberini S (2019) BTEX, nitrogen oxides, ammonia and ozone concentrations at traffic influenced and background urban sites in an arid environment. Atmos Pollut Res 10:445–454. https://doi.org/10.1016/j.apr.2018.08.009

Alipour M, Gupta VK, Massoudinejad M, Motahari S, Motesaddi Zarandi S (2021) Fabrication of silica aerogel and carbon–silica composite for dynamic adsorption of benzene from dry and wet gas streams. Int J Environ Anal:1–19. https://doi.org/10.1080/03067319.2021.1982921

Ansari KB, Danish M, Banerjee A, Hassan SZ, Sahayaraj DV, Khan MS, Huyen PT, Trinh QT (2022) Progress in biomass fast pyrolysis: an outlook of modern experimental approaches. In: Innovations in Thermochemical Technologies for Biofuel Processing. Elsevier, pp 21–62. https://doi.org/10.1016/B978-0-323-85586-0.00010-X

Antonucci A, Vitali M, Martellucci S, Mattei V, Protano C (2020) A cross-sectional study on benzene exposure in pediatric age and parental smoking habits at home. Int J Environ Res Public Health 17(15):5469. https://doi.org/10.3390/ijerph17155469

Baberi Z, Azhdarpoor A, Hoseini M, Baghapour M, Derakhshan Z, Giannakis S (2022) Monitoring benzene, toluene, ethylbenzene, and xylene (BTEX) levels in mixed-use residential-commercial buildings in Shiraz, Iran: Assessing the carcinogenicity and non-carcinogenicity risk of their inhabitants. Int J Environ Res Public Health 19(2):723. https://doi.org/10.3390/ijerph19020723

Bayatian M, Azari MR, Ashrafi K et al (2021) CFD simulation for dispersion of benzene at a petroleum refinery in diverse atmospheric conditions. Environ Sci Pollut Res 28:32973–32984. https://doi.org/10.1007/s11356-020-12254-1

Bedane AH, Guo TX, Eić M, Xiao H (2019) Adsorption of volatile organic compounds on peanut shell activated carbon. Can J Chem Eng 97(1):238–246. https://doi.org/10.1002/cjce.23330

Boro B, Paul R, Tan HL, Trinh QT, Rabeah J, Chang CC, Pao CW, Liu W, Nguyen NT, Mai BK, Mondal J (2023) Experimental validation and computational predictions join forces to map catalytic C–H activation in ferrocene metalated porous organic polymers. ACS Appl Mater Interfaces. https://doi.org/10.1021/acsami.3c01393

Chen G, Yang X, Ma Y, Ruan C, Chen Q, Jin X, Sun J, He S (2023) Structurally controllable hollow carbon spheres for gaseous benzene adsorption. J Environ Chem Eng 11(1):109182. https://doi.org/10.1016/j.jece.2022.109182

Chu B, Dada L, Liu Y, Yao L, Wang Y, Du W et al (2021) Particle growth with photochemical age from new particle formation to haze in the winter of Beijing, China. Sci Total Environ 753:142207. https://doi.org/10.1016/j.scitotenv.2020.142207

Danish M, Hashim R, Ibrahim MM, Sulaiman O (2014) Optimized preparation for large surface area activated carbon from date (*Phoenix dactylifera* L.) stone biomass. Biomass Bioenergy 61:167–178. https://doi.org/10.1016/j.biombioe.2013.12.008

De Jaegere T, Hein S, Claessens H (2016) A review of the characteristics of small-leaved lime (*Tilia cordata* Mill.) and their implications for silviculture in a changing climate. Forests 7(3):56. https://doi.org/10.3390/f7030056

Deng T, Shen X, Cheng X, Liu J (2021) Investigation of window-opening behaviour and indoor air quality in dwellings situated in the temperate zone in China. Indoor Built Environ 30(7):938–956. https://doi.org/10.1177/1420326X20924746

Directive 2008/50/EC of the European Parliament and of the Council of 21 May 2008 on Ambient Air Quality and Cleaner Air for Europe.

Djilani C, Zaghdoudi R, Modarressi A, Rogalski M, Djazi F, Lallam A (2012) Elimination of organic micropollutants by adsorption on activated carbon prepared from agricultural waste. Chem Eng J 189:203–212. https://doi.org/10.1016/j.cej.2012.02.059

Du Z, Mo J, Zhang Y, Xu Q (2014) Benzene, toluene and xylenes in newly renovated homes and associated health risk in Guangzhou, China. Build Environ 72:75–81. https://doi.org/10.1016/j.buildenv.2013.10.013

Fan R, Li J, Chen L, Xu Z, He D, Zhou Y, Zhu Y, Wei F, Li J (2014) Biomass fuels and coke plants are important sources of human exposure to polycyclic aromatic hydrocarbons, benzene and toluene. Environ Res 135:1–8. https://doi.org/10.1016/j.envres.2014.08.021

Fan X, Liao C, Bivolarova MP, Sekhar C, Laverge J, Lan L, Mainka A, Akimoto M, Wargocki P (2022) A field intervention study of the effects of window and door opening on bedroom IAQ, sleep quality, and next-day cognitive performance. Build Environ 225:109630. https://doi.org/10.1016/j.buildenv.2022.109630

Gayathiri M, Pulingam T, Lee KT, Sudesh K (2022) Activated carbon from biomass waste precursors: Factors affecting production and adsorption mechanism. Chemosphere:133764. https://doi.org/10.1016/j.chemosphere.2022.133764

Ge JC, Choi NJ (2017) Fabrication of functional polyurethane/rare earth nanocomposite membranes by electrospinning and its VOCs absorption capacity from air. Nanomaterials 7(3):60. https://doi.org/10.3390/nano7030060

Gupta M, Kumar A, Sharma S, Bharti Ghamouss F, Singh P, Chawla V, Kumar A, Kumar Y (2022) Study of electrochemical properties of activated carbon electrode synthesized using bio-waste for supercapacitor applications. Biomass Convers Biorefin:1–12. https://doi.org/10.1007/s13399-021-02271-6

Ha SH, Kim KH, Younis SA, Dou X (2020) The interactive roles of space velocity and particle size in a microporous carbon bed system in controlling adsorptive removal of gaseous benzene under ambient conditions. Chem Eng J 401:126010. https://doi.org/10.1016/j.cej.2020.126010

Hsieh PY, Shearston JA, Hilpert M (2021) Benzene emissions from gas station clusters: a new framework for estimating lifetime cancer risk. J Environ Health Sci Eng 19:273–283. https://doi.org/10.1007/s40201-020-00601-w

Hu J, Yu E, Liao Z (2021) Changes in cognitive function and related brain regions in chronic benzene poisoning: a case report. Ann Transl Med 9(1). https://doi.org/10.21037/atm-20-6597

Huang H, Huang H, Zhan Y, Liu G, Wang X, Lu H, Xiao L, Feng Q, Leung DY (2016) Efficient degradation of gaseous benzene by VUV photolysis combined with ozone-assisted catalytic oxidation: performance and mechanism. Appl Catal Environ 186:62–68. https://doi.org/10.1016/j.apcatb.2015.12.055

IARC (1987) Overall evaluations of carcinogenicity: an updating of IARC Monographs volumes 1 to 42 IARC Monogr Eval Carcinog Risks Hum Suppl. Supplement 7:40–41

Isinkaralar K (2023b) A study on the gaseous benzene removal based on adsorption onto the cost-effective and environmentally friendly adsorbent. Molecules 28(8):3453. https://doi.org/10.3390/molecules28083453

Isinkaralar K (2023c) Experimental evaluation of benzene adsorption in the gas phase using activated carbon from waste biomass. Biomass Convers Biorefin:1–10. https://doi.org/10.1007/s13399-023-03979-3

Isinkaralar O (2023a) Bioclimatic comfort in urban planning and modeling spatial change during 2020–2100 according to climate

change scenarios in Kocaeli, Türkiye. Int J Environ Sci Technol:1–12. https://doi.org/10.1007/s13762-023-04992-9

Isinkaralar O, Varol C (2023) A cellular automata-based approach for spatio-temporal modeling of the city center as a complex system: The case of Kastamonu, Türkiye. Cities 132:104073. https://doi.org/10.1016/j.cities.2022.104073

Istanbullu SN, Sevik H, Isinkaralar K, Isinkaralar O (2023) Spatial distribution of heavy metal contamination in road dust samples from an urban environment in Samsun, Türkiye. Bull Environ Contam Toxicol 110(4):78. https://doi.org/10.1007/s00128-023-03720-w

Jafari AJ, Kalantary RR, Esrafili A, Arfaeinia H (2018) Synthesis of silica-functionalized graphene oxide/ZnO coated on fiberglass and its application in photocatalytic removal of gaseous benzene. Process Saf Environ Prot 116:377–387. https://doi.org/10.1016/j.psep.2018.03.015

Janitz AE, Campbell JE, Magzamen S, Pate A, Stoner JA, Peck JD (2017) Benzene and childhood acute leukemia in Oklahoma. Environ Res 158:167–173. https://doi.org/10.1016/j.envres.2017.06.015

Janković B, Manić N, Dodevski V, Radović I, Pijović M, Katnić Đ, Tasić G (2019) Physico-chemical characterization of carbonized apricot kernel shell as precursor for activated carbon preparation in clean technology utilization. J Clean Prod 236:117614. https://doi.org/10.1016/j.jclepro.2019.117614

Jephcote C, Mah A (2019) Regional inequalities in benzene exposures across the European petrochemical industry: a Bayesian multilevel modelling approach. Environ Int 132:104812. https://doi.org/10.1016/j.envint.2019.05.006

Ji Y, Gao F, Wu Z, Li L, Li D, Zhang H, Zhang Y, Gao J, Bai Y, Li H (2020) A review of atmospheric benzene homologues in China: characterization, health risk assessment, source identification and countermeasures. J Environ Sci 95:225–239. https://doi.org/10.1016/j.jes.2020.03.035

Jiang B, Wen Y, Li Z, Xia D, Liu X (2018) Theoretical analysis on the removal of cyclic volatile organic compounds by non-thermal plasma. Water Air Soil Pollut 229:1–12. https://doi.org/10.1007/s11270-018-3687-3

Kadimpati KK, Sanneboina S, Golla N, Ayla S, Kumpati R, Skarka W (2020) Microalgae as an efficient feedstock biomass for biofuel production. Microbial Strat Techno-econ Biofuel Prod:129–169

Kadimpati KK, Thadikamala S, Devarapalli K, Banoth L, Uppuluri KB (2021) Characterization and hydrolysis optimization of Sargassum cinereum for the fermentative production of 3G bioethanol. Biomass Convers Biorefin 13:1831–1841. https://doi.org/10.1007/s13399-020-01270-3

Kang I, Xi J, Hu H (2018) Photolysis and photooxidation of typical gaseous VOCs by UV irradiation: removal performance and mechanisms. Front Environ Sci Eng 12(3):8. https://doi.org/10.1007/s11783-018-1032-0

Khalighi Sheshdeh R, Khosravi Nikou MR, Badii K, Mohammadzadeh S (2013) Evaluation of adsorption kinetics and equilibrium for the removal of benzene by modified diatomite. Chem Eng Technol 36(10):1713–1720. https://doi.org/10.1002/ceat.201300041

Konggidinata MI, Chao B, Lian Q, Subramaniam R, Zappi M, Gang DD (2017) Equilibrium, kinetic and thermodynamic studies for adsorption of BTEX onto Ordered Mesoporous Carbon (OMC). J Hazard Mater 336:249–259. https://doi.org/10.1016/j.jhazmat.2017.04.073

Kumar KK, Sujatha S, Skarka W, Monfort O (2023) An innovative hybrid biosorbent composed of nano ZnO and marine macro algae Jania rubens embedded in an alginate/PVA matrix: insights into Pb 2+ removal in water. New J Chem 47(1):373–383. https://doi.org/10.1039/D2NJ04896E

Laskar II, Hashisho Z, Phillips JH, Anderson JE, Nichols M (2019) Modeling the effect of relative humidity on adsorption dynamics of volatile organic compound onto activated carbon. Environ Sci Technol 53(5):2647–2659. https://doi.org/10.1021/acs.est.8b05664

Li X, Zhang L, Yang Z, Wang P, Yan Y, Ran J (2020) Adsorption materials for volatile organic compounds (VOCs) and the key factors for VOCs adsorption process: a review. Sep Purif Technol 235:116213. https://doi.org/10.1016/j.seppur.2019.116213

Li Y, Shen Y, Niu Z, Tian J, Zhang D, Tang Z, Li W (2023) Process analysis of temperature swing adsorption and temperature vacuum swing adsorption in VOCs recovery from activated carbon. Chin J Chem Eng 53:346–360. https://doi.org/10.1016/j.cjche.2022.01.029

Liu B, Younis SA, Kim KH (2021) The dynamic competition in adsorption between gaseous benzene and moisture on metal-organic frameworks across their varying concentration levels. Chem Eng J 421:127813. https://doi.org/10.1016/j.cej.2020.127813

Liu C, Huang X, Li J (2020) Outdoor benzene highly impacts indoor concentrations globally. Sci Total Environ 720:137640. https://doi.org/10.1016/j.scitotenv.2020.137640

Liu HB, Yang B, Xue ND (2016) Enhanced adsorption of benzene vapor on granular activated carbon under humid conditions due to shifts in hydrophobicity and total micropore volume. J Hazard Mater 318:425–432. https://doi.org/10.1016/j.jhazmat.2016.07.026

Luijten M, Ball NS, Dearfield KL, Gollapudi BB, Johnson GE, Madia F, Peel L, Pfuhler S, Settivari RS, ter Burg W, White PA, van Benthem J (2020) Utility of a next generation framework for assessment of genomic damage: a case study using the industrial chemical benzene. Environ Mol Mutagen 61(1):94–113. https://doi.org/10.1002/em.22346

Mao H, Huang R, Hashisho Z, Wang S, Chen H, Wang H, Zhou D (2016) Adsorption of toluene and acetone vapors on microwave-prepared activated carbon from agricultural residues: isotherms, kinetics, and thermodynamics studies. Res Chem Intermed 42:3359–3371. https://doi.org/10.1007/s11164-015-2217-9

Mohammed J, Nasri NS, Zaini MAA, Hamza UD, Ani FN (2015) Adsorption of benzene and toluene onto KOH activated coconut shell based carbon treated with NH3. Int Biodeter Biodegr 102:245–255. https://doi.org/10.1016/j.ibiod.2015.02.012

Nasrullah A, Saad B, Bhat AH, Khan AS, Danish M, Isa MH, Naeem A (2019) Mangosteen peel waste as a sustainable precursor for high surface area mesoporous activated carbon: characterization and application for methylene blue removal. J Clean Prod 211:1190–1200. https://doi.org/10.1016/j.jclepro.2018.11.094

Norbäck D, Hashim JH, Hashim Z, Ali F (2017) Volatile organic compounds (VOC), formaldehyde and nitrogen dioxide (NO2) in schools in Johor Bahru, Malaysia: associations with rhinitis, ocular, throat and dermal symptoms, headache and fatigue. Sci Total Environ 592:153–216. https://doi.org/10.1016/j.scitotenv.2017.02.215

Oginni O, Singh K, Oporto G, Dawson-Andoh B, McDonald L, Sabolsky E (2019) Effect of one-step and two-step H3PO4 activation on activated carbon characteristics. Bioresour Technol Rep 8:100307. https://doi.org/10.1016/j.biteb.2019.100307

Oliva G, Comia JJR, Senatore V, Zarra T, Ballestreros F, Belgiorno V, Naddeo V (2022) Degradation of gaseous volatile organic compounds (VOCs) by a novel UV-ozone technology. Sci Rep 12(1):11112. https://doi.org/10.1038/s41598-022-14191-0

Orru H, Idavain J, Pindus M, Orru K, Kesanurm K, Lang A, Tomasova J (2018) Residents' self-reported health effects and annoyance in relation to air pollution exposure in an industrial area in Eastern-Estonia. Int J Environ Res Public Health 15:252. https://doi.org/10.3390/ijerph15020252

OSHA (1987) Occupational exposure to benzene: final rule, September 11, Part II. Fed Regist 52:34460–34578

Paul R, Shit SC, Fovanna T, Ferri D, Srinivasa Rao B, Gunasooriya GKK, Dao DQ, Le QV, Shown I, Sherburne MP, Trinh QT, Mondal J (2020) Realizing catalytic acetophenone hydrodeoxygenation with palladium-equipped porous organic polymers. ACS Appl Mater Interfaces 12(45):50550–50565. https://doi.org/10.1021/acsami.0c16680

Rajabi H, Mosleh MH, Prakoso T, Ghaemi N, Mandal P, Lea-Langton A, Sedighi M (2021) Competitive adsorption of multicomponent volatile organic compounds on biochar. Chemosphere 283:131288. https://doi.org/10.1016/j.chemosphere.2021.131288

Rajamanickam R, Baskaran D, Kaliyamoorthi K, Baskaran V, Krishnan J (2020) Steady State, transient behavior and kinetic modeling of benzene removal in an aerobic biofilter. J Environ Chem Eng 8(2):103657. https://doi.org/10.1016/j.jece.2020.103657

Rashid J, Tehreem F, Rehman A, Kumar R (2019) Synthesis using natural functionalization of activated carbon from pumpkin peels for decolourization of aqueous methylene blue. Sci Total Environ 671:369–376. https://doi.org/10.1016/j.scitotenv.2019.03.363

Reffas A, Bernardet V, David B, Reinert L, Lehocine MB, Dubois M, Batisse N, Duclaux L (2010) Carbons prepared from coffee grounds by H_3PO_4 activation: characterization and adsorption of methylene blue and Nylosan Red N-2RBL. J Hazard Mater 175(1-3):779–788. https://doi.org/10.1016/j.jhazmat.2009.10.076

Ren J, Wang J, Guo X, Zhang W, Chen Y, Gao A (2022) Lnc-TC/miR-142-5p/CUL4B signaling axis promoted cell ferroptosis to participate in benzene hematotoxicity. Life Sci 310:121111. https://doi.org/10.1016/j.lfs.2022.121111

Rich AL, Orimoloye HT (2016) Elevated atmospheric levels of benzene and benzene-related compounds from unconventional shale extraction and processing: human health concern for residential communities. Environ Health Insights 10:75–82. https://doi.org/10.4137/EHI.S33314

Rubahamya B, Kumar Reddy KS, Prabhu A, Al Shoaibi A, Srinivasakannan C (2019) Porous carbon screening for benzene sorption. Environ Prog Sustain Energy 38(1):93–99. https://doi.org/10.1002/ep.12925

Sarkar C, Pendem S, Shrotri A, Dao DQ, Pham Thi Mai P, Nguyen Ngoc T, Chandaka DR, Rao TV, Trinh QT, Sherburne MP, Mondal J (2019) Interface engineering of graphene-supported Cu nanoparticles encapsulated by mesoporous silica for size-dependent catalytic oxidative coupling of aromatic amines. ACS Appl Mater Interfaces 11(12):11722–11735. https://doi.org/10.1021/acsami.8b18675

Seku K, Gangapuram BR, Pejjai B, Hussain M, Hussaini SS, Golla N, Kadimpati KK (2019) Eco-friendly synthesis of gold nanoparticles using carboxymethylated gum Cochlospermum gossypium (CMGK) and their catalytic and antibacterial applications. Chem Papers 73:1695–1704. https://doi.org/10.1007/s11696-019-00722-z

Shi G, He S, Chen G, Ruan C, Ma Y, Chen Q, Jin X, Liu X, He C, Du C, Dai H, Yang X (2022) Crayfish shell-based micro-mesoporous activated carbon: insight into preparation and gaseous benzene adsorption mechanism. Chem Eng J 428:131148. https://doi.org/10.1016/j.cej.2021.131148

Singh BP, Sohrab SS, Athar M, Alandijany TA, Kumari S, Nair A, Kumari S, Mehra K, Chowdhary K, Rahman S, Azhar EI (2023) Substantial changes in selected volatile organic compounds (VOCs) and associations with health risk assessments in industrial areas during the COVID-19 pandemic. Toxics 11(2):165. https://doi.org/10.3390/toxics11020165

Singuru R, Trinh QT, Banerjee B, Govinda Rao B, Bai L, Bhaumik A, Reddy BM, Hirao H, Mondal J (2016) Integrated experimental and theoretical study of shape-controlled catalytic oxidative coupling of aromatic amines over CuO nanostructures. ACS omega 1(6):1121–1138. https://doi.org/10.1021/acsomega.6b00331

Spinelle L, Gerboles M, Kok G, Persijn S, Sauerwald T (2017) Review of portable and low-cost sensors for the ambient air monitoring of benzene and other volatile organic compounds. Sensors 17(7):1520. https://doi.org/10.3390/s17071520

Sun P, Guo X, Chen Y, Zhang W, Duan H, Gao A (2018a) VNN3, a potential novel biomarker for benzene toxicity, is involved in 1, 4-benzoquinone induced cell proliferation. Environ Pollut 233:323–330. https://doi.org/10.1016/j.envpol.2017.10.087

Sun P, Zhang J, Liu W, Wang Q, Cao W (2018b) Modification to LH kinetics model and its application in the investigation on photodegradation of gaseous benzene by nitrogen-doped TiO2. Catalysts 8(8):326. https://doi.org/10.3390/catal8080326

Sun Y, Hou J, Cheng R, Sheng Y, Zhang X, Sundell J (2019) Indoor air quality, ventilation and their associations with sick building syndrome in Chinese homes. Energ Buildings 197:112–119. https://doi.org/10.1016/j.enbuild.2019.05.046

Szulejko JE, Kim KH, Parise J (2019) Seeking the most powerful and practical real-world sorbents for gaseous benzene as a representative volatile organic compound based on performance metrics. Sep Purif Technol 212:980–985. https://doi.org/10.1016/j.seppur.2018.11.001

Trinh QT, Nguyen AV, Huynh DC, Pham TH, Mushrif SH (2016) Mechanistic insights into the catalytic elimination of tar and the promotional effect of boron on it: first-principles study using toluene as a model compound. Cat Sci Technol 6(15):5871–5883. https://doi.org/10.1039/C6CY00358C

Tuli FJ, Hossain A, Kibria AF, Tareq ARM, Mamun SM, Ullah AA (2020) Removal of methylene blue from water by low-cost activated carbon prepared from tea waste: a study of adsorption isotherm and kinetics. Environ Nanotechnol Monit Manag 14:100354. https://doi.org/10.1016/j.enmm.2020.100354

Tunsaringkarn T, Siriwong W, Rungsiyothin A, Nopparatbundit S (2012) Occupational exposure of gasoline station workers to BTEX compounds in Bangkok. Thailand Int J Occup Environ Med 3:117–125

US EPA (1999) Determination of volatile organic compounds in ambient air using active sampling onto sorbent tubes, compendium of methods for the determination of toxic organic compounds in ambient air, Second Edition Compendium Method TO-17. U.S. Environmental Protection Agency (US EPA)

Ushiki I, Ota M, Sato Y, Inomata H (2015) VOCs (acetone, toluene, and n-hexane) adsorption equilibria on mesoporous silica (MCM-41) over a wide range of supercritical carbon dioxide conditions: experimental and theoretical approach by the Dubinin–Astakhov equation. Fluid Phase Equilibria 403:78–84. https://doi.org/10.1016/j.fluid.2015.06.019

Valencia A, Muñiz-Valencia R, Ceballos-Magaña SG, Rojas-Mayorga CK, Bonilla-Petriciolet A, González J, Aguayo-Villarreal IA (2022) Cyclohexane and benzene separation by fixed-bed adsorption on activated carbons prepared from coconut shell. Environ Technol Innov 25:102076. https://doi.org/10.1016/j.eti.2021.102076

Vikrant K, Kim KH, Peng WX, Ge SB, Ok YS (2020) Adsorption performance of standard biochar materials against volatile organic compounds in air: a case study using benzene and methyl ethyl ketone. Chem Eng J 387:123943. https://doi.org/10.1016/j.cej.2019.123943

Vohra MS (2015) Adsorption-based removal of gas-phase benzene using granular activated carbon (GAC) produced from date palm pits. Arab J Sci Eng 40(11):3007–3017. https://doi.org/10.1007/s13369-015-1683-0

Wang G, Dou B, Zhang Z, Wang J, Liu H, Hao Z (2015) Adsorption of benzene, cyclohexane and hexane on ordered mesoporous carbon. J Environ Sci 30:65–73. https://doi.org/10.1016/j.jes.2014.10.015

Wang X, Cheng H, Ye G, Fan J, Yao F, Wang Y, Jiao Y, Zhu W, Huang H, Ye D (2022) Key factors and primary modification methods

of activated carbon and their application in adsorption of carbon-based gases: a review. Chemosphere 287:131995. https://doi.org/10.1016/j.chemosphere.2021.131995

Wang YH, Bayatpour S, Qian X, Frigo-Vaz B, Wang P (2021) Activated carbon fibers via reductive carbonization of cellulosic biomass for adsorption of non-polar volatile organic compounds. Colloids Surf A Physicochem Eng Asp 612:125908. https://doi.org/10.1016/j.colsurfa.2020.125908

WHO (2021) Global Air Quality Guidelines. In: Particulate Matter, Ozone, Nitrogen Dioxide, Sulfur Dioxide and Carbon Monoxide, vol 2021. World Health Organization, Geneva

Wjihi S, Erto A, Knani S, Lamine AB (2017) Investigation of adsorption process of benzene and toluene on activated carbon by means of grand canonical ensemble. J Mol Liq 238:402–410. https://doi.org/10.1016/j.molliq.2017.04.021

Xie LH, Liu XM, He T, Li JR (2018) Metal-organic frameworks for the capture of trace aromatic volatile organic compounds. Chem 4(8):1911–1927. https://doi.org/10.1016/j.chempr.2018.05.017

Yang P, Li J, Zuo S (2017) Promoting oxidative activity and stability of CeO2 addition on the MnOx modified kaolin-based catalysts for catalytic combustion of benzene. Chem Eng Sci 162:218–226. https://doi.org/10.1016/j.ces.2017.01.009

Yao X, Liu Y, Li T, Zhang T, Li H, Wang W, Shen X, Qian F, Yao Z (2020) Adsorption behavior of multicomponent volatile organic compounds on a citric acid residue waste-based activated carbon: experiment and molecular simulation. J Hazard Mater 392:122323. https://doi.org/10.1016/j.jhazmat.2020.122323

Ye W, Zhang X, Gao J, Cao GY, Zhou X, Su X (2017) Indoor air pollutants, ventilation rate determinants and potential control strategies in Chinese dwellings: a literature review. Sci Total Environ 586:697–729. https://doi.org/10.1016/j.scitotenv.2017.02.047

Yu H, Lin F, Li K, Wang W, Yan B, Song Y, Chen G (2021) Triple combination of natural microbial action, etching, and gas foaming to synthesize hierarchical porous carbon for efficient adsorption of VOCs. Environ Res 202:111687. https://doi.org/10.1016/j.envres.2021.111687

Yu W, Deng L, Yuan P, Liu D, Yuan W, Chen F (2015) Preparation of hierarchically porous diatomite/MFI-type zeolite composites and their performance for benzene adsorption: the effects of desilication. Chem Eng J 270:450–458. https://doi.org/10.1016/j.cej.2015.02.065

Zaitan H, Manero MH, Valdés H (2016) Application of high silica zeolite ZSM-5 in a hybrid treatment process based on sequential adsorption and ozonation for VOCs elimination. J Environ Sci 41:59–68. https://doi.org/10.1016/j.jes.2015.05.021

Zhang X, Cao J, Wei J, Zhang Y (2018) Improved C-history method for rapidly and accurately measuring the characteristic parameters of formaldehyde/VOCs emitted from building materials. Build Environ 143:570–578. https://doi.org/10.1016/j.buildenv.2018.07.030

Zhang X, Gao B, Creamer AE, Cao C, Li Y (2017) Adsorption of VOCs onto engineered carbon materials: a review. J Hazard Mater 338:102–123. https://doi.org/10.1016/j.jhazmat.2017.05.013

Zhao Z, Ma S, Gao B, Bi F, Qiao R, Yang Y, Wu M, Zhang X (2023) A systematic review of intermediates and their characterization methods in VOCs degradation by different catalytic technologies. Sep Purif Technol 123510. https://doi.org/10.1016/j.seppur.2023.123510

Zhou K, Ma W, Zeng Z, Ma X, Xu X, Guo Y, Li H, Li L (2019) Experimental and DFT study on the adsorption of VOCs on activated carbon/metal oxides composites. Chem Eng J 372:1122–1133. https://doi.org/10.1016/j.cej.2019.04.218

Zhu L, Shen D, Luo KH (2020) A critical review on VOCs adsorption by different porous materials: species, mechanisms and modification methods. J Hazard Mater 389:122102. https://doi.org/10.1016/j.jhazmat.2020.122102

Zhu R, Yu Q, Li M, Zhao H, Jin S, Huang Y, Fan J, Chen J (2021) Analysis of factors influencing pore structure development of agricultural and forestry waste-derived activated carbon for adsorption application in gas and liquid phases: a review. J Environ Chem Eng 9(5):105905. https://doi.org/10.1016/j.jece.2021.105905